Inorg. Chem. **2002**, *41*, 6056–6061

Isolation of the New Cubic Phases $RE_4FeGa_{12-x}Ge_x$ (RE = Sm, Tb; x = 2.5) from Molten Gallium: Single-Crystal Neutron Diffraction Study of the Ga/Ge Distribution

Marina A. Zhuravleva,[†] Xiaoping Wang,[‡] Arthur J. Schultz,[‡] Thomas Bakas,[§] and Mercouri G. Kanatzidis*,[†]

Department of Chemistry, Michigan State University, East Lansing, Michigan 48824, Intense Pulse Neutron Source, Argonne National Laboratory, Argonne, Illinois 60439, and University of Ioannina, Ioannina, Greece 45110

Received February 18, 2002

The compounds $RE_4FeGa_{12-x}Ge_x$ (RE = Sm, Tb) were discovered in reactions employing molten Ga as a solvent at 850 °C. However, the isostructural $Y_4FeGa_{12-x}Ge_x$ was prepared from a direct combination reaction. The crystal structure is cubic with space group $Im\bar{3}m$, Z = 2, and a = 8.657(4) Å and 8.5620(9) Å for the Sm and Tb analogues, respectively. Structure refinement based on full-matrix least squares on F_o^2 resulted in R_1 = 1.47% and wR_2 = 4.13% [$I > 2\sigma(I)$] for RE = Sm and R_1 = 2.29% and wR_2 = 7.12% [$I > 2\sigma(I)$] for RE = Tb. The compounds crystallize in the $U_4Re_7Si_6$ structure type, where the RE atoms are located on *8c* (1/4, 1/4, 1/4) sites and the Fe atoms on *2a* (0, 0, 0) sites. The distribution of Ga and Ge in the structure, investigated with single-crystal neutron diffraction on the Tb analogue, revealed that these atoms are disordered over the *12d* (1/4, 0, 1/2) and *12e* (x, 0, 0) sites. The amount of Ga/Ge occupying the *12d* and *12e* sites refined to 89(4)/11 and 70(4)/30%, respectively. Transport property measurements indicate that these compounds are metallic conductors. Magnetic susceptibility measurements and Mössbauer spectroscopy performed on the Tb analogue show a nonmagnetic state for Fe, while the Tb atoms carry a magnetic moment corresponding to a μ_{eff} of 9.25 μ_B.

Introduction

Crystal growth employing molten metals[1] and molten salts[2] has been known for a long time; however their use in deliberate solid-state synthesis has attracted increasing attention in recent years.[3−5] Because of the huge potential for new materials discovery in the realm of intermetallics, the molten metal flux technique is proving to be an outstanding tool for exploration.[6−10] The advantages of this method lie in the enhanced diffusion of the elements facilitated by the solvent and the lower reaction temperatures that can be tolerated. The latter allow better kinetic control that gives

* To whom correspondence should be addressed. E-mail: kanatzid@cem.msu.edu.
[†] Michigan State University.
[‡] Argonne National Laboratory.
[§] University of Ioannina.

(1) Deitch, R. H. In *Crystal Growth*; Pamplin, B. R., Ed.; Pergamon Press: Oxford, New York, 1975. Lundström, T. *J. Less-Common Met.* **1984**, *100*, 215−228. Canfield, P. C.; Fisk, Z. *Philos. Mag. B* **1992**, *65*, 1117−1123.
(2) Elwell, D.; Scheel, H. J. *Crystal growth from high-temperature solutions*; Academic Press: London, New York, 1975.
(3) Kanatzidis, M. G.; Sutorik, A. *Prog. Inorg. Chem.* **1995**, *43*, 151−265. Kanatzidis, M. G. *Curr. Opin. Solid State Mater. Sci.* **1997**, *2*, 139−149.
(4) Schaefer, J.; Bluhm, K. *Z. Anorg. Allg. Chem*. **1994**, *620*, 1578−1582; Utzolino, A.; Bluhm, K. Z. *Naturforsch., B: Chem. Sci.* **1996**, *51* (*3*), 305−308. Luce, J. L.; Schaffers, K. I.; Keszler, D. A. *Inorg. Chem.* **1994**, *33* (*11*), 2453−2455. Carpenter, J. D.; Hwu, S.-J. *Inorg. Chem*. **1995**, *34* (*18*), 4647−4651.
(5) DiSalvo, F. J. *Solid State Commun*. **1997**, *102*, 79−85.
(6) Rühl, R.; Jeitschko, W. *Inorg. Chem.* **1982**, *21*, 1886−1891. Niemann, S.; Jeitschko, W. J. *Solid State Chem.* **1995**, *114*, 337−341. Niemann, S.; Jeitschko, W. J. *J. Alloys Compd.* **1995**, *221*, 235−239. Ebel, T.; Jeitschko, W. *J. Solid State Chem.* **1995**, *116*, 307−313. Kaiser, P.; Jeitschko, W. *J. Solid State Chem.* **1996**, *124*, 346−352. Okada, S.; Suda, T.; Kamezaki, A.; et al.. *Mater. Sci. Eng., A* **1996**, *209*, 33−37. Thiede, V. M. T.; Fehrmann, B.; Jeitschko, W. Z. *Anorg. Allg. Chem.* **1999**, *625*, 1417−1425.
(7) Chen, X. Z.; Sieve, B.; Henning, R.; Schultz, A. J.; Brazis, P.; Kannewurf, C. R.; Cowen, J. A.; Crosby, R.; Kanatzidis, M. G. *Angew. Chem., Intl. Ed.* **1999**, *38*, 693−696.
(8) Chen, X. Z.; Spourtouch, S.; Brazis, P.; Kannewurf, C. R.; Cowen, J. A.; Patschke, R.; Kanatzidis, M. G. *Chem. Mater*. **1998**, *10*, 3202−3211.
(9) Sieve, B.; Chen, X. Z.; Cowen, J. A.; Larson, P.; Mahanti. S. D.; Kanatzidis, M. G. *Chem. Mater*. **1999**, *11*, 2451−2455.
(10) Sieve, B.; Sportouch, S.; Chen, X, Z.; Cowen, J. A.; Brazis, P.; Kannewurf, C. R.; Papaefthymiou, V.; Kanatzidis, M. G. *Chem. Mater*. **2001**, *13*, 273−283.

10.1021/ic025544b CCC: $22.00
Published on Web 10/22/2002

more flexibility to adopt novel compositions and atomic arrangements in the structure. Recently, we suggested the use of liquid Al for the synthesis of new Si- and Ge-containing materials and have reported on the $Ho_2Al_3Si_2$,[7] $Sm_2Ni(Si_{1-x}Ni_x)Al_4Si_6$,[8] $RENiAl_4Ge_2$[9] (RE = Sm, Tb, Y), $RE_4Fe_{2+x}Al_{7-x}Si_8$[10] (RE = Ce, Pr, Nd, Sm), and $RE_8Ru_{12}Al_{49}Si_9(Al_xSi_{12-x})$[11] (RE = Pr, Sm). The success of molten Al to uncover new materials stimulated us to explore the related Ga system. The known binary and ternary compounds of Ga are numerous;[12] however, there is still a paucity of data on quaternary intermetallic phases such as silicides and germanides. Using liquid Ga we have already discovered $SmNiSi_3$, $YNiSi_3$,[13] and Sm_2NiGa_{12}.[14] Our continued investigations with Ga targeting quaternary silicides and germanides focused on the systems RE/M/Ga/Ge (RE = Y, Ce, Sm, Gd, Tb; M = Fe, Co, Ni, Cu). Here we report preliminary results regarding the Fe system and describe the synthesis, crystal structure, and transport and magnetic properties of the cubic phases $RE_4FeGa_{12-x}Ge_x$.

Experimental Section

Synthesis. Rare earth, Fe, and Ge were combined with a large excess of Ga under a nitrogen atmosphere. Alumina crucibles containing the reaction mixtures Sm (Tb) (3.6 mmol), Fe (0.9 mmol), Ge (2.7 mmol), and Ga (27 mmol) were placed into silica tubes and sealed under high vacuum $<1 \times 10^{-4}$ Torr. The heating profile included slow heating (60 °C/h) up to 1000 °C, a short isothermal step at 1000 °C to allow proper homogenization, cooling (75 °C/h) to 850 °C, and long isothermal step 72 h at 850 °C. The system was then allowed to cool slowly (15 °C/h) to ~200−250 °C, and the tubes were taken out for hot-filtration to remove liquid Ga. The filtration was done using specially designed silica filters with coarse frit by centrifuging at high speed > 3000 rpm for approximately 30 s. After filtration the residual Ga flux was removed with ~3 M solution of I_2 in dimethylformamide (DMF) overnight. The resultant crystalline product was subsequently washed in DMF and hot water and dried by washing with acetone and ether. The product was $RE_4FeGa_{12-x}Ge_x$ as a major phase (about 75%) and $FeGa_3$ and Ge as minor phases. For RE = Sm, the formation of the ternary phase Sm_3Ga_9Ge[15] was also observed.

EDS Analysis. The micrographs of the samples were taken with a scanning electron microscope (SEM) JEOL JSM-35C. A semi-quantitative elemental analysis by energy dispersive spectroscopy (EDS) was done on the SEM equipped with an EDS detector. The analysis was conducted at accelerating voltage 20 kV and collection time 30 s. Data were taken from several samples, and the results were averaged. The EDS analysis shows that the elemental composition of the samples under investigation corresponds to the formula $RE_3FeGa_8Ge_3$. The composition was consistent for both Sm and Tb analogues, despite the complication caused by partial overlap of energies of Fe Kα line (6.403 keV) and Tb Lα lines (6.272 keV) in the X-ray fluorescence spectra.

Table 1. Crystal and Structure Refinement Data for $RE_4FeGa_6Ge_6$ (RE = Sm, Tb)

empirical formula	$Sm_4Fe_{1+y}Ga_6Ge_{6-y}$ ($y = 1$)	$Tb_4FeGa_6Ge_6$
fw	1493.98	1545.39
temp (K)	298	298
wavelength (Å)	0.71 073	0.71 073
space group	$Im\bar{3}m$ (No. 229)	$Im\bar{3}m$ (No. 229)
lattice constants (Å)	$a = 8.657(4)$	$a = 8.5620(9)$
V (Å^3)	648.7(6)	627.66(11)
Z	2	2
calcd density (g/cm^3)	7.684	8.177
abs coeff (mm^{-1})	43.496	50.017
F(000)	1292	1328
final R indices $[I > 2\sigma(I)]$[a]	$R_1 = 0.0147$, $wR_2 = 0.0413$	$R_1 = 0.0229$, $wR_2 = 0.0712$
R indices (all data)	$R_1 = 0.0161$, $wR_2 = 0.0417$	$R_1 = 0.0234$, $wR_2 = 0.0713$
extinction coeff	0.001 41(12)	0.0024(3)

[a] $R_1 = \Sigma| |F_o| - |F_c| |/\Sigma|F_o|$; $wR_2 = [w\{|F_o| - |F_c|\}^2/w|F_o|^2]^{1/2}$, $w = 1/\sigma^2\{|F_o|\}$.

Table 2. Atomic Coordinates ($\times 10^4$) and Equivalent Isotropic Displacement Parameters (Å$^2 \times 10^3$) for $RE_4FeGa_6Ge_6$ (RE = Sm, Tb)[a,b]

atom	Wykoff symbol	x	y	z	U(eq)	occ
Fe	2a	0	0	0	10(1)	1.0
	2a	0	0	0	10(1)	1.0
Sm	8c	2500	2500	2500	9(1)	1.0
Tb	8c	2500	2500	2500	8(1)	1.0
M(1)	12d	2500	0	5000	10(1)	1.0 Ga
	12d	2500	0	5000	9(1)	1.0 Ga
M(2)	12e	2882(2)	0	0	9(1)	0.83(4) Ge + 0.16(5) Fe
	12e	2882(2)	0	0	10(1)	1.0 Ge

[a] $U_{(eq)}$ is defined as one-third of the trace of the orthogonalized $\mathbf{U}_{ij}$ tensor. [b] First and second lines correspond to RE = Sm and Tb, respectively.

Single-Crystal X-ray Crystallography. Single-crystal X-ray diffraction data were collected at room temperature on a Siemens Platform SMART CCD diffractometer. The samples of size $0.06 \times 0.06 \times 0.04$ mm^3 for RE = Sm and $0.1 \times 0.16 \times 0.02$ mm^3 for RE = Tb were cut from larger crystals and mounted on glass fibers. A hemisphere of data (Mo Kα radiation, $\lambda = 0.710\,73$ Å) was acquired using exposure time 60 s/frame for Sm and 30 s/frame for Y and Tb analogues. The data collection and acquisition were done with the SMART[16] software package, and the SAINTPLUS[17] program was used for data reduction. An empirical correction for absorption based on symmetry equivalent reflections was applied using SADABS. Systematic absences led to the following possible space groups: $I23$; $I2_13$; $Im\bar{3}$; $I432$, $I\bar{3}m$; $Im\bar{3}m$. The highest symmetry space group $Im\bar{3}m$ was chosen. The structures were solved with direct methods and refined using the full-matrix least-squares technique with the SHELXTL software package. Details of the data collection and structure refinement are listed in Table 1. The final atomic positions, the equivalent thermal displacement parameters and occupancies are given in Table 2. The interatomic distances up to 3.5 Å are listed in Table 3.

In the structure a total of four atomic sites for RE (*8c*; 1/4, 1/4, 1/4), Fe (*2a*; 0, 0, 0), Ga (*12d*; 1/4, 0, 1/2), and Ge (*12e*; *x*, 0, 0), one for each element, were identified. For the Sm analogue a mixed occupancy of Fe with Ge was observed on the *12e* crystallographic site. It is not possible however to distinguish between Ga and Ge atoms relying on X-ray diffraction data only. The R-values and the values of the resulting thermal displacement parameters were

(11) Sieve, B.; Chen, X. Z.; Henning, R.; Brazis, P.; Kannevurf, C. R.; Cowen, J. A.; Schultz, A. J.; Kanatzidis, M. G. *J. Am. Chem. Soc.* **2001**, *29*, 7040−7047.
(12) Grin', Yu. N.; Gladyshevskii, R. E. *Gallides Handbook*; Metallurgy: Moscow, 1989 (in Russian).
(13) Chen, X. Z.; Larson, P.; Sportouch, S.; Brazis, P.; Mahanti, S. D.; Kannewurf, C. R.; Kanatzidis, M. G. *Chem. Mater.* **1999**, *11*, 75−83.
(14) Chen, X. Z.; Small, P.; Zhuravleva, M.; Brazis, P.; Kannewurf, C. R.; Kanatzidis, M. G. *Chem. Mater*. **2000**, *12*, 2520−2522.
(15) Zhuravleva, M.; Kanatzidis, M. G. *J. Solid State Chem.* **2002**, in press.
(16) *SMART*, version 5; Siemens Analytical X-ray Systems, Inc.: Madison, WI, 1998.
(17) *SAINT*, version 4; Siemens Analytical X-ray Systems, Inc.: Madison, WI, 1994−96.

Table 3. Bond Lengths (Å) for $RE_4FeGa_6Ge_6$ (RE = Sm, Tb)[a]

bond	dist (Å)	multiplicity
M(2)−M(1)	2.8381(17)	×4
	2.8125(17)	×4
Sm−M(2)	3.0781(15)	×6
Tb−M(2)	3.0436(4)	×6
Sm−M(1)	3.0606(15)	×6
Tb−M(1)	3.0271(3)	×6
M(2)−Fe	2.492(2)	×6
	2.457(3)	×6

[a] First and second lines correspond to RE = Sm and Tb, respectively.

entirely satisfactory for the assignment of Ga atoms to *12d* and Ge to *12e* positions. However, the resulting formula $RE_4FeGa_6Ge_6$ is in disagreement with the composition given by EDS: $RE_4FeGa_8Ge_3$. Thus, the uncertainty about the Ga/Ge distribution motivated us to undertake a single-crystal neutron diffraction crystallographic analysis. In contrast to the small difference in X-ray scattering lengths (~3%) between Ga and Ge atoms, the neutron scattering lengths for Ga and Ge atoms differ significantly (~10%). Thus neutron diffraction provides a better means for distinguishing these two elements in a crystalline sample.

Single-Crystal Neutron Crystallography. Neutron diffraction data were collected from a single crystal of $Tb_4FeGa_{12-x}Ge_x$ weighing 30.1 mg (2.3 × 2.3 × 1.8 mm^3) at the Intense Pulse Neutron Source (IPNS), Argonne National Laboratory, on the single-crystal diffractometer (SCD). A detailed description of the SCD instrument and data collection and analysis procedures has been published.[18,19] An autoindexing algorithm[20] was used to obtain an initial orientation matrix from the peaks in one histogram. For intensity data collection, a total of 18 histograms were measured—each for a different crystal setting. Bragg peaks were integrated in three dimensions about their predicted locations and were corrected for the incident neutron spectrum, detector efficiency and dead-time loss. Lorenz and absorption corrections were also applied. The GSAS software package[21] was used for structural analysis. The initial coordinates were based on the single-crystal X-ray diffraction.

The refinement based on the original assignment of Ga at *12d* and Ge at *12e* positions yielded $R(F)/R_w(F) = 0.068/0.083$ and slightly enlarged thermal displacement parameter for Ge. After introduction of a mixed occupancy model between Ga/Ge in both *12d* and *12e* sites (with occupancy refinement), the resulting R-values dropped and the temperature factor of the *12e* site improved. Occupancies of the Ga and Ge atoms were found to be 0.89(4) for Ga(1) and 0.11(4) for Ge(1) at *12d* and 0.70(4) for Ga(2) and 0.30(4) for Ge(2) at *12e*. All atoms were refined with anisotropic atomic displacement parameters, and the final refinement converged to $R(F) = 0.062$ and $R_w(F) = 0.073$. The resulting formula $Tb_4FeGa_{9.54}Ge_{2.46}$ is in fair agreement with EDS elemental analysis. A summary of parameters related to the neutron diffraction analysis is presented in Table 4. Atomic coordinates and site occupancies are listed in Table 5.

Magnetic Properties and Mössbauer Spectroscopy. The magnetization of 33.0 mg of a single-crystal sample of $Tb_4FeGa_{12-x}Ge_x$ was measured in the temperature range 2−300 K with an applied external field of 500 G using a Quantum Design MPMS SQUID magnetometer. The field dependence of the magnetic susceptibility was examined up to fields of ±1 T at 2 K. Raw susceptibility data were corrected for the sample holder contribution.

Table 4. Crystal Data and Structural Refinement Parameters for $Tb_4FeGa_{9.54}Ge_{2.46}$ Obtained from Neutron Diffraction

formula	$Tb_4FeGa_{9.5(3)}Ge_{2.5(3)}$
fw	1535.325
temp (K)	298(2)
cryst system	cubic
space group	$Im\bar{3}m$
a (Å)	8.6054(6)
V ($Å^3$)	637.25(8)
Z	2
d_{calc} (g cm^{-3})	8.002
size (mm^3)	2.3 × 2.3 × 1.8
radiation	neutrons
data collcn technique	time-of-flight Laue
$\mu(\lambda)$ (cm^{-1})	$0.393 + 0.2223\lambda$
reflcns collcd ($I > 3\sigma(I)$)	1454
params refined	34
refinement method	full-matrix least squares on F
R indices $R_w(F)$,[a] $R(F)$[b]	0.073, 0.062
goodness-of-fit	1.49

[a] $Rw(F) = \{\Sigma[w(F_o - F_c)^2]/\Sigma[w(F_o)^2]\}^{1/2}$. [b] $R(F) = \Sigma||F_o| - |F_c||/\Sigma|F_o|$.

Table 5. Fractional Atomic Coordinates for $Tb_4FeGa_{9.5(3)}Ge_{2.5(3)}$

atom	site sym	x	y	z	occ.	U(eq) ($Å^2$)
Fe(1)	2a	0.0000	0.0000	0.0000	1.0	0.0101
Tb(1)	8c	0.2500	0.2500	0.2500	1.0	0.0085
M(1)	12d	0.2500	0.0000	0.5000	0.89(4) Ga + 0.11(4) Ge	0.0091
M(2)	12e	0.28378	0.0000	0.0000	0.70(4) Ga + 0.30(4) Ge	0.0101

The Mössbauer spectra were taken on polycrystalline sample of $Tb_4FeGa_{12-x}Ge_x$ with a constant-acceleration spectrometer, equipped with a ^{57}Co source in Rh matrix. The spectrometer was calibrated with metallic iron, and the isomer shift values are reported relative to α-Fe. A closed-loop refrigerator system was used for the low-temperature measurements. An Oxford Instrument Variox 316 cryostat was used for measurements at liquid-helium temperature.

Results and Discussion

Synthesis. The compounds $RE_4FeGa_{12-x}Ge_x$ were discovered from reactions in liquid Ga involving RE, M and Ge, where RE is Y, Ce, Sm, Gd, and Tb and M is Fe, Co, Ni, and Cu. These systems were investigated at various metal ratios and different heating regimes. A heating regime with a shorter isothermal step was shown to favor the formation of cubic phases $RE_4FeGa_{12-x}Ge_x$. For example, when a 6 day isothermal step (T = 850 °C) was used in the system Tb/Fe/Ga/Ge, the products were Tb_4FeGe_8 and $Tb_2Ga_2Ge_5$,[22] along with the cubic phase as a minor product. The shorter isothermal step of 3 days at 850 °C, on the other hand, produced the cubic phase in high yield. For RE = Sm, the situation was similar, as the 6 day isothermal heating gave rise to Sm_3Ga_9Ge as the major component and the cubic phases $FeGa_3$ and Ge as minor components. Reducing the time by half brought about an increase in the yield of the cubic phase. From this we conclude that the cubic phases are essentially kinetic products of the reaction.

It is interesting that we did not observe isostructural phases as M was changed from Co to Ni or to Cu. Instead, a variety of other quaternary compounds[23,24] were detected. In addition,

(18) Schultz, A. J.; Van Derveer, D. G.; Parker, D. W.; Baldwin, J. E. *Acta Crystallogr., Sect. C* **1990**, *C46*, 276.
(19) Schultz, A. J. *Trans. Am. Cryst. Assoc*. **1993**, *29*, 29.
(20) Jacobson, R. A. *J. Appl. Crystallogr*. **1986**, *19*, 283.
(21) Larson, A. C.; Von Dreele R. B. *GSAS General Structural Analysis System*; Los Alamos National Laboratory: Los Alamos, NM, 2000.

(22) The Tb_4FeGe_8, crystallizes in the supercell of $CeNiSi_2$ structure type, and the $Tb_2Ga_2Ge_5$ phase crystallizes in the Ce_2GaGe_6 structure type. Zhuravleva, M. A.; Kanatzidis, M. G. Unpublished results.

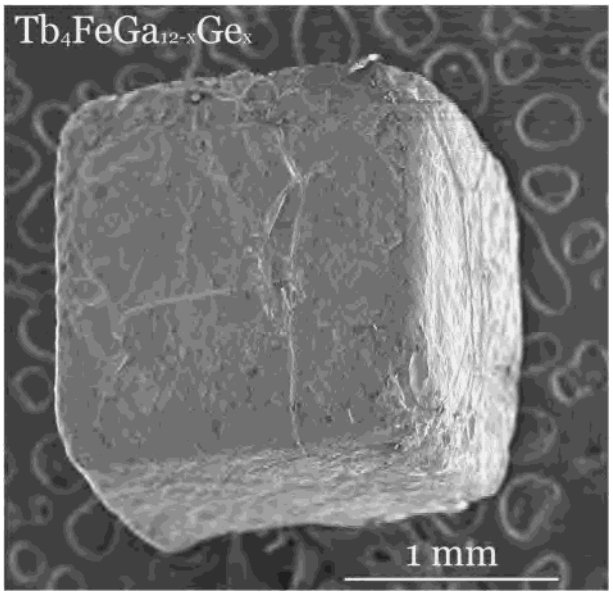

Figure 1. SEM image of a typical Ga-grown $Tb_4FeGa_{12-x}Ge_x$ crystal. The roughening of the surface is caused by an etching process during isolation.

the type of RE appears to be important in phase formation. Thus, in the system RE/Fe/Ga/Ge, when RE was Y, Ce, and Gd, the ternary RE_3Ga_9Ge[15] phases were predominantly found. Remarkably, the Y analogue $Y_4FeGa_{12-x}Ge_x$[25] does exist; however, it was obtained from a direct combination reaction. It is unclear at this point whether the analogues of $RE_4FeGa_{12-x}Ge_x$, with RE other than Y, Sm, and Tb, are unstable or the window of proper experimental synthetic conditions for these is rather narrow and was not accessed in this study.

Unlike conventional solid-state techniques used for the synthesis of isostructural to $U_4Re_7Si_6$-type compounds (see below), the molten metal method enables the faster diffusion of the elements in the reaction mixture and promotes crystal growth. Thus, large single crystals of $Tb_4FeGa_{12-x}Ge_x$, measuring up to 2 mm each side, could be grown from molten Ga; see Figure 1. The incorporation of Ga in these phases shows that in this case the solvent is reactive. This is in contrast to the Sm/Ni/Ga/Si system in which the Ga-free $SmNiSi_3$ phase could be obtained.

Crystal Structure. The $RE_4FeGa_{12-x}Ge_x$ compounds crystallize in the $U_4Re_7Si_6$[26] structure type. This is a rather stable structural arrangement as a large number of isotypic ternary phases with Sc,[27] lanthanides,[28,29] and actinides,[30] as well as group IVA metals,[31] are known. The $RE_4FeGa_{12-x}Ge_x$ species seem to be the first quaternary analogues of the $U_4Re_7Si_6$ structure type. The general formula for these compounds could be written as $A_4M(M'_6T_6)$, where A = Sc, Ln, Ac, Zr, and Hf, M = transition metal, M′ = transition metal or Ga, and Tt = tetrelide or Ga. The examples of those are $Sc_4M_7Ge_6$,[27] $RE_4M_7Ge_6$[28] (M = Ru, Os, Rh, Ir), U_4Tc_7Tt (Tt = Si, Ge), $Np_4Ru_7Ge_6$,[30] $U_4Re_7Si_6$ and $M_4Co_7Ge_6$[31] (M = Zr, Hf), and even RE_4MGa_{12}[29] (RE = Ho, Tm; M = Ni, Pd).

The position of the transition metal in the structure of these compounds is rather interesting: it could occupy only one crystallographic position with the lowest multiplicity (*2a*; 0, 0, 0), as it is for $RE_4FeGa_{12-x}Ge_x$ and RE_4MGa_{12}, or two positions (*2a*, 0, 0, 0; *12d*, 1/4, 0, 1/2), as it is in all other cases reported earlier. There seems to be a tendency that if the compound does not contain a group III element (e.g. Ga), the two sites are occupied with transition metal. However, in the presence of Ga, the transition metal adopts only the lowest multiplicity site, while the higher multiplicity site becomes preferably stabilized with Ga. In effect, as we can see in the example of Tm_4NiGa_{12}, Ga could occupy both the transition metal and a tetrelide position.

The structure of $Sm_4FeGa_{12-x}Ge_x$ viewed along the [001] direction is depicted in Figure 2A. The red spheres represent Sm atoms, the green spheres are Fe atoms, and the mixed occupied positions M(1) = Ga(1)/Ge(1) and M(2) = Ga(2)/Ge(2) are drawn in blue and yellow, respectively. This structure, as shown, is rather complicated; however, it becomes clearer when described in polyhedral representation. The two types of polyhedra found in this structure are shown in Figure 2B. The first, drawn in green, are the atoms of Fe octahedraly coordinated within 2.495(2) Å to six M(2) atoms. The second, drawn in blue, is a highly distorted tetrahedron of $M(1)M(2)_4$ with M(1) atom in the center and M(2) atoms in its corners. The distortion occurs in a way that two out of six edges are short (3.667 Å) and four are long (5.046 Å). In this structure the tetrahedra share their edges forming a three-dimensional $[Ga_{12-x}Ge_x]$ substructure; see Figure 2C. The $FeM(2)_6$ octahedra occupy every corner and the center of the cubic unit cell, sharing their corners with the $[Ga_{12-x}Ge_x]$ framework, as shown in Figure 2D. The octahedra are not connected with each other, and the closest distance between two apical M(2) atoms is about 3.66 Å. The Sm atoms are situated in the pockets formed by $Fe[Ge_{12-x}Ge_x]$ substructure at the positions *8c* (1/4, 1/4, 1/4); see Figure 2E.

Another way to view this structure is to subdivide it into two slabs, one of which is shown in Figure 2F. The superposition of this slab on an identical one, but shifted by the centering operation to (1/2 1/2 1/2), will produce the whole structure. As seen from Figure 2F, the Sm atoms form an ideal cubic framework, in which the Sm−Sm distance is

(23) Zhuravleva, M. A.; Chen, X. Z.; Wang, X.; Schultz, A. J.; Ireland, J.; Kannewurf, C. R.; Kanatzidis, M. G. *Chem. Mater*. **2002**, *14*, 3066−3081.
(24) Zhuravleva, M. A.; Pcionek, R. J.; Kanatzidis, M. G. Manuscript in preparation.
(25) $Y_4FeGa_{12-x}Ge_x$: space group $Im\bar{3}m$, $Z = 2$, cell parameter $a = 8.5683(12)$ Å. Single-crystal X-ray structure refinement based on full-matrix least squares on F_o^2 resulted in $R_1 = 2.64\%$ and $wR_2 = 8.15\%$ [$I > 2\sigma(I)$].
(26) Aksel'rud, L. G.; Yarmolyuk, Ya. P.; Gladyshevskii, E. I. *Dopov. Akad. Nauk Ukr. RSR, Ser. A* **1978**, *40* (4), 359−362.
(27) Engel, N.; Chabot, B.; Parté, E. *J. Less-Common Met.* **1984**, *96*, 291.
(28) Francois, M.; Venturini, G.; Mareche, J. F.; Malaman, B.; Roques, B. *J. Less-Common Met.* **1985**, *113*, 231.
(29) Vasilenko, L. O.; Noga, A. S.; Grin', Yu. N.; Koterlin, M. D.; Yarmolyuk, Ya. P. Russian Metallurgy; translated from: *Izv. Akad. Nauk SSSR, Met.* **1988**, *5*, 216−220.
(30) Wastin, F.; Rebizant, J.; Sanchez, J. P.; Blaise, A.; Goffart, J.; Spirlet, J. C.; Walker, C. T.; Fuger, J. *J. Alloys Compd.* **1994**, *210*, 83.
(31) Zubrik, O. I.; Olenich, R. R.; Yarmolyuk, Ya. P. *Dopov. Akad. Nauk Ukr. RSR, Ser. A* **1982**, *11*, 74.

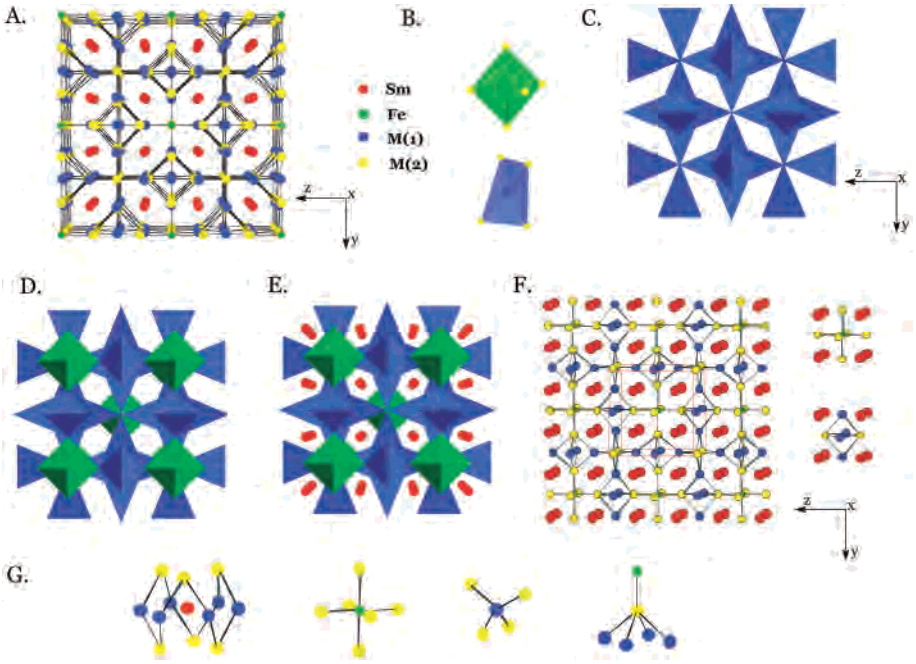

Figure 2. Structure of $Sm_4FeGa_{12-x}Ge_x$: (A) view along the [100] direction; (B) $FeM(2)_6$ and $M(1)M(2)_4$ polyhedra; (C) $[Ga_{12-x}Ge_x]$ framework in polyhedral representation; (D) polyhedral representation of $Fe[Ga_{12-x}Ge_x]$ substructure; (E) $Sm_4FeGa_{12-x}Ge_x$ structure in polyhedral representation; (F) $Sm_4FeGa_{12-x}Ge_x$ structure in ball-and-stick representation; (G) local coordination environment of Sm, Fe, and M(1) = Ga(1)/Ge(1) and M(2) = Ga(2)/Ge(2) atoms.

4.328 Å, exactly half the unit cell period of 8.657(4) Å. Thus, each unit cell consists of eight cubes made of Sm atoms. Every fourth of such cube contains the $FeM(2)_6$ octahedra, having Fe atoms in the center of the cube and M(2) atoms at the center of the faces. Three out of four Sm cubes of the unit cell do not have any atom in the center, but the centers of four faces of the cube are occupied with M(1) type of atoms, forming the base of the square bypyramid. The empirical formula of the unit cell content comprised by two types of cubes is then $[SmFeM(2)_6] \times 1 + [SmM(1)_2] \times 3 = Sm_4FeM(1)_6M(2)_6 = Sm_4FeGa_{12-x}Ge_x$, $Z = 2$.

We also point out that this structure can be thought as stuffed (and therefore distorted) form of the $AuCu_3$ [Au_4Cu_{12}] structure, where the Au atoms occupy the RE atom position in the $RE_4FeGa_{12-x}Ge_x$ structure and the Cu atoms occupy the Ga and Ge positions. The Fe atom can be thought of as an interstitial, sitting in only a fraction of the octahedral pockets.

The local coordinations of the Sm (within 3.5 Å), Fe, and disordered Ga/Ga atoms M(1) and M(2) (within 3.0 Å) are shown in Figure 2G. The Sm atom has 12 neighbors in its immediate coordination sphere. These include six M(1) atoms within 3.0606(15) Å in a form of a flat hexagon (with the Sm is the center) and six additional M(2) atoms with three located below and three above the hexagon in a trigonal antiprismatic geometry (the Sm−M(2) distance is 3.0784(15) Å). The Fe atoms are in a perfect octahedral environment of six M(2) atoms at 2.492(2) Å. The next nearest to M(2) atoms are Sm located at 3.75 Å. The M(1) atom is in the distorted tetrahedral environment of M(2) atoms. The M(2) atoms are bonded to four M(1) atoms in the form of a square pyramid, defined by a base of four M(1) atoms and an apex of an Fe atom. For a list of selected bond distances, see Table 3.

Physical Properties. Seebeck coefficient measurements done on single crystals of $Tb_4FeGa_{12-x}Ge_x$ show an extremely low value of thermopower, which is a characteristic of metallic conductors. The thermopower is on the order of ±2 μV/K and stays low in the entire temperature range of 50−400 K.[32]

The magnetic properties of $Tb_4FeGa_{12-x}Ge_x$ were studied, and a plot of the temperature-dependent magnetic susceptibility and the inverse magnetic susceptibility, calculated per mole of Tb, is shown in Figure 3A. At low temperatures, a maximum in the magnetic susceptibility, T_{max}, is observed at 12 K, indicative of antiferromagnetic ordering. As the temperature drops below the T_{max} of 12 K, the difference in the zero-field-cooled (ZFC) and field-cooled (FC) part of susceptibility becomes substantial; see Figure 3B. The Néel temperature $T_N = 13.0$ K was obtained from a set of the isofield $\chi_{mol}T$ measurements, as shown in Figure 4.

Above T_N the magnetic susceptibility follows Curie−Weiss behavior, as given in the linear $(\chi_{mol})^{-1}$ vs T plot, with a Weiss constant of −48 K. The effective magnetic moment μ_{eff}, calculated from the slope of the line and normalized per one Tb atom, gave a value of 9.25 μ_B. This is in a good agreement with the one calculated using the Van Vleck equation[33] for a free Tb^{3+} atom, $\mu_{eff} = 9.72$ μ_B, showing that the RE atoms in the structure are in a +3 state, whereas the Fe atoms do not contribute to the magnetic susceptibility. The field dependence of the magnetic moment measured at 2 K did not exhibit any hysteresis and stays linear up to the fields of ±1 T.

(32) The Seebeck coefficient of a single-crystal sample of $Tb_4FeGa_{12-x}Ge_x$ was measured between 50 and 400 K by using a SB-100 Seebeck Effect Measurement System from MMR Technologies.

(33) Van Vleck, J. H. *The Theory of Electric and Magnetic Susceptibilities*; Oxford University Press: Oxford, U.K., 1932.

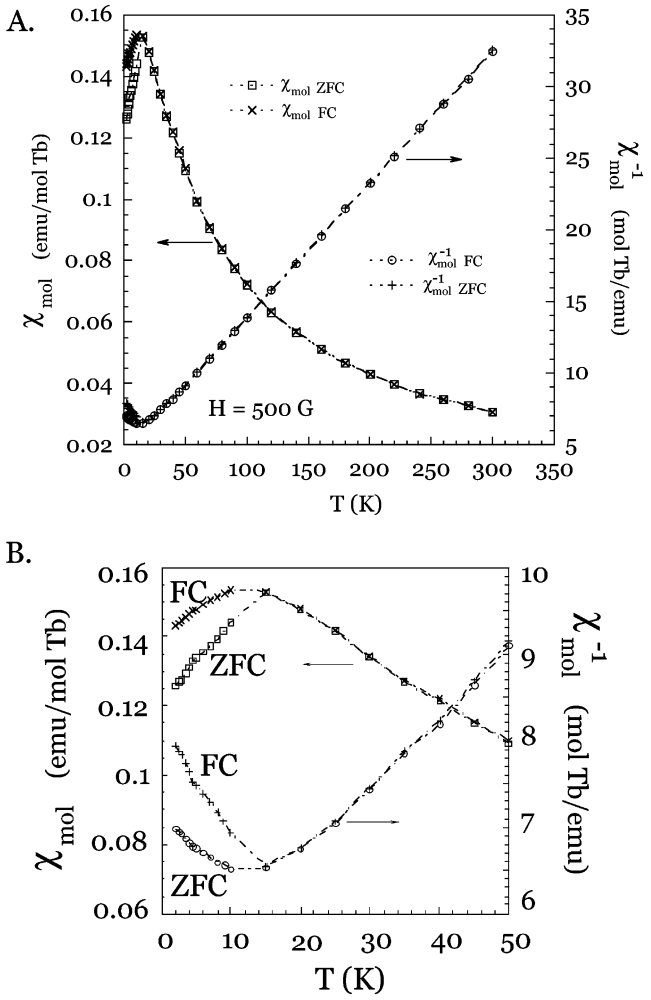

Figure 3. (A) Temperature dependence of the molar magnetic susceptibility and the inverse molar magnetic susceptibility of $Tb_4FeGa_{12-x}Ge_x$. (B) Magnetic susceptibility near the maximum.

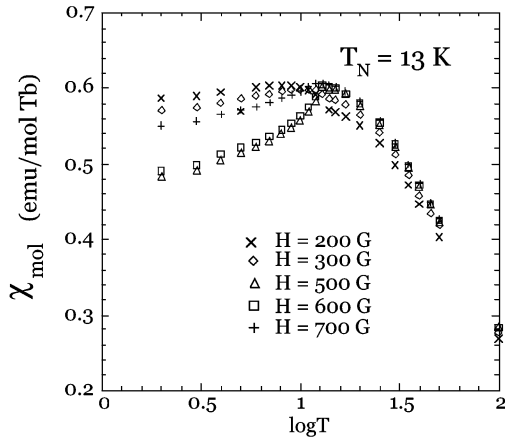

Figure 4. Isofield temperature dependence of the magnetic susceptibility of $Tb_4FeGa_{12-x}Ge_x$.

The nonmagnetic state of Fe atoms was also confirmed with ^{57}Fe Mössbauer spectroscopy taken at 4.2 and 18 K. The 18 K spectrum fitted in Lorentzian form is shown in Figure 5. Two components were identified with hyperfine parameters: isomer shift, ∂ (0.56 mm/s, 0.41 mm/s); quadrupole splitting, ΔE_q (0.17 mm/s, 0.26 mm/s); relative areas (85%, 15%). The larger area subcomponent with the lower

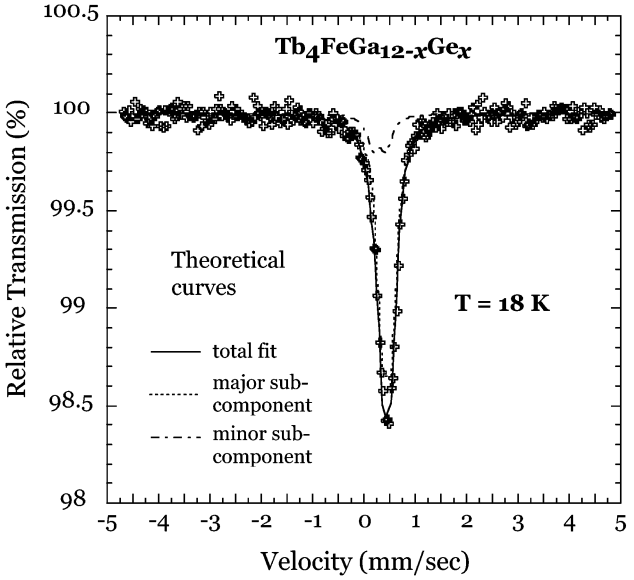

Figure 5. ^{57}Fe Mössbauer spectrum of $Tb_4FeGa_{12-x}Ge_x$ at 18 K. The solid line is the least-squares fit of the experimental data.

value of quadrupole splitting reflects the fact that Fe is in perfect octahedral environment of Ga atoms. Because the coordination sphere of Fe atoms also contains some Ge atoms partially occupying the Ga position, the symmetry of this particular local Fe sites is slightly lowered. The disorder between Ga and Ge may be responsible for the appearance of the minor subcomponent with higher value of ΔE_q. No indication is observed in the spectra taken at 18 and 4.2 K for magnetic splitting due to ordering of magnetic moments centered on Fe atoms. Similar nonmagnetic character of the Fe atoms was observed in the intermetallic compounds $RE_4Fe_{2+x}Al_{7-x}Si_8$.[10]

Concluding Remarks

Exploratory synthesis in the system RE/M/Ga/Ge (RE = Y, Ce, Sm, Gd, Tb; M = Fe, Co, Ni, Cu) with the liquid Ga as a solvent gave rise to new compounds of the general formula $RE_4FeGa_{12-x}Ge_x$ (RE = Sm, Tb). The formation of isostructural phases was not observed for M = Co, Ni, or Cu, suggesting that Fe is critical to the stabilization of these cubic phases. The $RE_4FeGa_{12-x}Ge_x$ species are the first quaternary analogues of the cubic $U_4Re_7Si_6$ structure type and contain a three-dimensional $[Ga_{12-x}Ge_x]$ framework, which accommodates Fe in octahedral pockets and RE atoms in the remaining 3D voids. The rare-earth atoms are in a +3 formal oxidation state whereas the Fe atoms are in nonmagnetic state. Antiferromagnetic ordering of spins localized on Tb atoms occurs at the Néel temperature of 13 K.

Acknowledgment. Financial support from the Department of Energy (Grant No. DE-FG02-99ER45793) is gratefully acknowledged. This work made use of the SEM facilities of the Center for Advanced Microscopy at Michigan State University.

Supporting Information Available: X-ray crystallographic files, in CIF format. This material is available free of charge via the Internet at http://pubs.acs.org.

IC025544B